Metallicity and physical conditions in the Magellanic Bridge

Lehner, N., Howk, J. C., Keenan, F., & Smoker, J. V. (2008). Metallicity and physical conditions in the Magellanic Bridge. The Astrophysical Journal, 678(1), 219-233. DOI: 10.1086/529574

Published in:
The Astrophysical Journal

Document Version:
Publisher's PDF, also known as Version of record

The Astrophysical Journal, 678:219–233, 2008 May 1

METALLICITY AND PHYSICAL CONDITIONS IN THE MAGELLANIC BRIDGE[1]

N. Lehner,[2] J. C. Howk,[2] F. P. Keenan,[3] and J. V. Smoker[3]

Received 2007 July 19; accepted 2008 January 16

ABSTRACT

We present a new analysis of the diffuse gas in the Magellanic Bridge (R.A. $\gtrsim 3^h$) based on *HST* STIS E140M and *FUSE* spectra of two early-type stars lying within the Bridge and a QSO behind it. We derive the column densities of the H I (from Lyα), N I, O I, Ar I, Si II, S II, and Fe II of the gas in the Bridge. Using the atomic species, we determine the first gas-phase metallicity of the Magellanic Bridge, $[Z/\mathrm{H}] = -1.02 \pm 0.07$ toward one sight line and $-1.7 < [Z/\mathrm{H}] < -0.9$ toward the other, a factor of 2 or more smaller than the present-day SMC metallicity. Using the metallicity and $N(\mathrm{H\ I})$, we show that the Bridge gas along our three lines of sight is $\sim$70%–90% ionized, despite high H I columns, $\log N(\mathrm{H\ I}) \simeq 19.6-20.1$. Possible sources for the ongoing ionization are certainly the hot stars within the Bridge, hot gas (revealed by O VI absorption), and leaking photons from the SMC and LMC. From the analysis of C II*, we deduce that the overall density of the Bridge must be low (<0.03–$0.1\ \mathrm{cm}^{-3}$). We argue that our findings combined with other recent observational results should motivate new models of the evolution of the SMC-LMC-Galaxy system.

Subject headings: galaxies: abundances — ISM: structure — Magellanic Clouds — ultraviolet: ISM

1. INTRODUCTION

The evolution of galaxies is closely coupled with the interactions between them. Encounters between galaxies are frequent and were certainly habitual in the early epoch of galaxy formation (e.g., Barnes & Hernquist 1992; Larson & Tinsley 1978; Maller et al. 2006). These encounters reshape the galaxies, transfer mass, energy, and metals between them, and may even create new sites of star formation within the newly produced gaseous features between the galaxies or new bursts of star formation in the colliding galaxies (Larson & Tinsley 1978; Barton et al. 2007; de Mello et al. 2008). These galactic interactions are not believed to be major contributors to the pollution of the intergalactic medium (e.g., Aguirre et al. 2001), but they nonetheless affect the metal content and physics of the galaxies themselves and their halos, and therefore the evolution of the galaxies and their surroundings.

In our Galactic neighborhood, interactions between the Magellanic Clouds and the Galaxy are believed to have produced several large gaseous features: the Magellanic Bridge (the Bridge), linking the Small Magellanic Cloud (SMC) and the Large Magellanic Cloud (LMC); the Magellanic Stream; and the Leading Arm, apparently linking the Clouds and our Galaxy (e.g., Mathewson et al. 1974; Putman 2000; Brüns et al. 2005). The Bridge is believed to have been produced through an interaction between the SMC and LMC, while the Stream and Leading Arm may have arisen through an interaction between the Galaxy and the Clouds (e.g., Gardiner & Noguchi 1996), although the origin of these latter gaseous features is far from settled (Nidever et al. 2008; Besla et al. 2007). The proximity of these gaseous features and the global view of the Magellanic System with little line-of-sight confusion allow us to study the result of interacting galaxies in a way not otherwise possible. The Bridge is the focus of the present work.

In the past few years, multiwavelength observations of the Bridge have revealed some key characteristics. Radio H I observations have shown that approximately two-thirds of the H I gas surrounding the Clouds is found in the Bridge, while only 25% and 6% are found in the Stream and the Leading Arm, respectively (Brüns et al. 2005). Some of the Bridge gas even appears to build up and feed the Stream via an interface region (Brüns et al. 2005). Far-UV observations have shown multiple gas phases in the Bridge, including not only the well-known neutral gas but also a significant amount of ionized gas and a small H_2 content (Lehner et al. 2001; Lehner 2002; this paper). Dense molecular clouds were also subsequently identified in the form of CO (Muller et al. 2003; Mizuno et al. 2006; although these CO surveys were realized in the SMC Wing, a much denser region of the Bridge in stars and gas content). Optical studies have revealed massive hot stars throughout the Bridge (Demers & Battinelli 1998). The ages of these stars are $\sim$10–40 Myr, implying that star formation is ongoing within the Bridge gas, since these stars could not migrate from the SMC during their lifetimes, although Harris (2007) suggests that star formation in the Bridge may have been more important 200–300 Myr ago.

The *N*-body numerical simulation of the Galaxy-SMC-LMC system by Gardiner & Noguchi (1996) reproduced some of the observed characteristics of the Bridge (principally, the H I column density and velocity distributions), along with those of the Stream. In this paper, we still use their numerical simulation as a basis, although we note that the hypotheses and validity of this model and other recent numerical simulations (e.g., Yoshizawa & Noguchi 2003) have been recently brought into question in view of the new *Hubble Space Telescope* (*HST*) measurements of the proper motions of the LMC and SMC (Kallivayalil et al. 2006a, 2006b; Besla et al. 2007; and see § 5.3). Gardiner & Noguchi's model predicts that the Bridge was formed from tidally stripped gas pulled from the SMC during a close encounter between the SMC and the LMC some 200 Myr ago. The new calculations of the LMC and SMC orbits still suggest that the closest approach between these two galaxies occurred some 200 Myr ago (Kallivayalil et al. 2006a), and therefore the new proper motions may only affect the interpretation of the origins of the

[1] Based on observations made with the NASA-CNES-CSA *Far Ultraviolet Spectroscopic Explorer*. *FUSE* is operated for NASA by The Johns Hopkins University under NASA contract NAS5-32985. Based on observations made with the NASA/ESA *Hubble Space Telescope*, obtained at the Space Telescope Science Institute, which is operated by the Association of Universities for Research in Astronomy, Inc., under NASA contract NAS5-26555.

[2] Department of Physics, University of Notre Dame, 225 Nieuwland Science Hall, Notre Dame, IN 46556.

[3] Astrophysics Research Centre, School of Mathematics and Physics, Queen's University of Belfast, Belfast, UK.

Stream and Leading Arm. Nevertheless, there appear to be some challenges to these models.

Tidal models predict that both gas and stars are pulled from the SMC, and yet the search for an old stellar population in the Bridge has so far failed (Harris 2007). Furthermore, material pulled from the SMC should have a metallicity somewhat similar to that of the SMC some 200 Myr ago. But this appears to be in conflict with the B-type star abundances in the Bridge that imply an extremely low Bridge metallicity, −1.1 dex from solar (Rolleston et al. 1999; Lee et al. 2005), a factor of 3 and 5 metal deficiency for the SMC and LMC, respectively. The metallicity in the sparse regions of the Bridge is also at odds with that measured in the SMC Wing, also known as the western end of the Bridge, where the metallicity of B-type stars is found to be SMC-like (Lee et al. 2005). These metallicity estimates complicate the origin of the Bridge and suggest different evolutions or origins for the sparse and dense stellar regions of the Bridge.

An estimate of the present-day metallicity of the Bridge that is independent of stellar measurements is therefore critical. In this work, we present an estimate of the absolute gas-phase abundances of the Bridge toward two stars situated in relatively low H I column density regions. We compare the column densities of the neutral species (N I, O I, and Ar I) observed in absorption in the Space Telescope Imaging Spectrograph (STIS) and *Far Ultraviolet Spectroscopic Explorer* (*FUSE*) spectra to those for H I Lyα lines toward two early-type stars; i.e., our metallicity estimate is mostly independent of ionization correction. The Bridge Lyα absorption is heavily blended with the Galactic component, but we show that it is feasible to retrieve the Bridge H I column density. Using the metallicity and the amount of H I along these sight lines, we can for the first time quantify the amount of ionized gas in the Bridge; ionized gas is revealed to be a major component of the Bridge, yet this gas phase is mostly ignored in numerical simulations.

Our paper is organized as follows. In § 2 we briefly discuss the previous STIS and *FUSE* observations and the new *FUSE* observations of DGIK 975 and DI 1388. In § 3 we discuss our measurements of the metals and the H I column densities. We present in § 4 the first metallicity estimate of the Bridge gas and the fraction of neutral, ionized, and molecular gas. From the C II* diagnostic, we estimate the electron density and cooling rate in the Bridge. In § 5 we discuss our results (in particular, we address the possible origins of the low-metallicity and ionization sources of the Bridge) and the current observational challenges to the numerical simulations. Finally, in § 6 we summarize our key findings.

2. OBSERVATIONS

In Figure 1 we show the locations of our targets on an H I map of the Magellanic System from Brüns et al. (2005; more properties about the stars can be found in Lehner 2002). DI 1388 and PKS 0312−77 are situated approximately midway between the SMC and LMC, and DGIK 975 lies at the eastern end of the Bridge near the LMC halo, allowing us to probe different regions of the Bridge (see Fig. 1). All these sight lines are outside the SMC Wing that is approximately delimited by the box in Figure 1.

The two stars were observed with *FUSE*, the *HST* STIS E140M, and the 3.9 m Anglo-Australian Telescope (AAT). The QSO PKS 0312−77 was observed with the STIS E140M and *FUSE*, but the STIS and *FUSE* data are of too poor quality for a detailed metal-line absorption analysis. Unfortunately, the *FUSE* program F018 (PI: N. Lehner), intended to obtain a good-quality far-UV spectrum of this QSO, was not completed before the failure of *FUSE*, and only 16% of the requested time was observed. However, the STIS data can be rebinned and used to study the Lyα absorption. For the STIS E140M and AAT observations of DGIK 975 and DI 1388, we refer the reader to Lehner et al. (2001) and Lehner (2002). The previous *FUSE* observations of these two stars are also described in Lehner (2002). New *FUSE* observations were obtained for DI 1388 (program U106, nonproprietary reobservations of science targets) and DGIK 975 (program G050, PI: N. Lehner), adding another 10 and 29 ks exposure time, respectively. (Note that the total time for program U106 is 30 ks, but about half the exposures have no signal.) The total *FUSE* exposure times are therefore 28 ks for DI 1388 and 52 ks for DGIK 975.

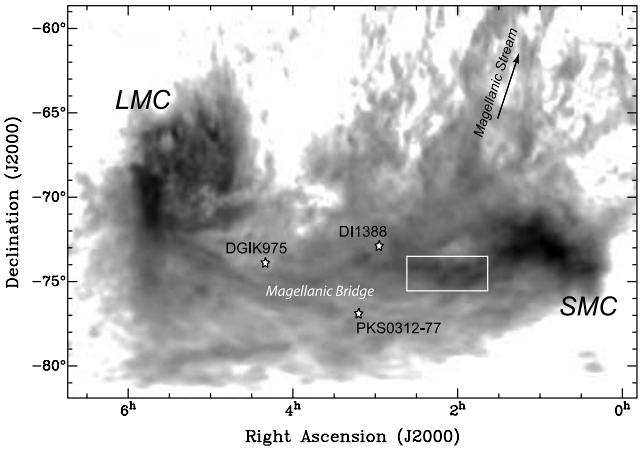

FIG. 1.—Location of our targets superimposed on the H I column density distribution from Brüns et al. [2005; darker regions represent higher N(H I); see Brüns et al. for the detailed N(H I) scale]. Our sight lines and major features of the Magellanic System are indicated. The box highlights a region known as the SMC Wing, or the western end of the Bridge.

All the *FUSE* data were recalibrated using the newest CALFUSE version (3.2; Dixon et al. 2007). The extracted spectra associated with the separate exposures were aligned by cross-correlating the positions of absorption lines and then co-added. The oversampled *FUSE* spectra were binned to a bin size of 0.027 Å (4 pixels), providing about three samples per ∼20 km s^{-1} resolution element. In order to achieve the optimum signal-to-noise ratio, segments with overlapping wavelengths were co-added for the DGIK 975 *FUSE* spectra. However, we ensured before co-adding the various spectra that none of the absorption lines of interest were affected by fixed-pattern noise by comparing the interstellar profiles in multiple detector segments. The zero point in the final *FUSE* wavelength scale was established by shifting the average *FUSE* velocity to the STIS 140M velocity of the same species (e.g., O I, N I, and Fe II). STIS data reduction provides excellent wavelength calibration, with a velocity uncertainty of ∼1 km s^{-1}.

3. ANALYSIS

3.1. *Metals*

The continuum levels near the metal-absorption lines were modeled by fitting Legendre polynomials within about [−300, 600] km s^{-1} of each absorption line. Low-order polynomials were generally adopted, but in some cases high-order polynomials were necessary (e.g., Fe III is blended with the stellar photospheric and wind lines). For weak lines, several continuum placements were tested to be certain that the continuum error was robust (see Sembach & Savage 1992). In Figures 2 and 3 we show the normalized spectra for the interstellar metal-line transitions in

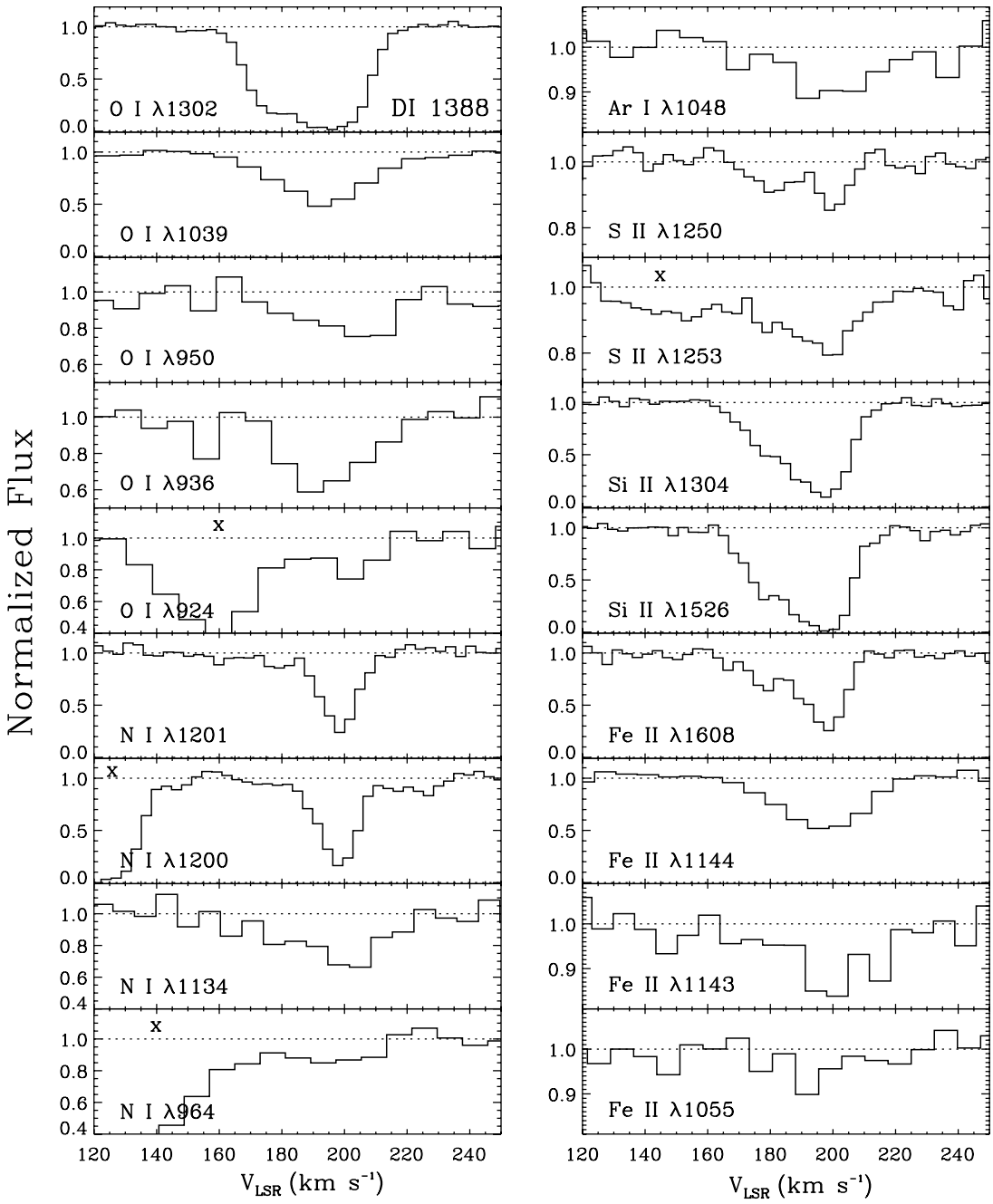

FIG. 2.—Normalized profiles against the LSR velocity near the Bridge velocities of neutral and singly ionized species in the STIS E140M and *FUSE* spectra of DI 1388. The Bridge absorption occurs between about 160 and 220 km s^{-1} toward this line of sight. The cross shows the part of the spectrum that is contaminated by other absorbing features.

DI 1388 and DGIK 975, respectively (see also Lehner et al. 2001; Lehner 2002). The selected transitions have no serious blends with other features.

In order to estimate the column density, we adopted the apparent optical depth (AOD) method of Savage & Sembach (1991). In this method the absorption profiles are converted into apparent column densities per unit velocity $N_a(v) = 3.768 \times 10^{14} \ln[F_c/F_{\rm obs}(v)]/(f\lambda)$ cm^{-2} (km s^{-1})$^{-1}$, where F_c is the continuum flux, $F_{\rm obs}(v)$ is the observed flux as a function of velocity, f is the oscillator strength of the absorption, and λ is in Å (atomic parameters were adopted from Morton 2003). The total column density was obtained by integrating over the absorption profile $N_a = \int N_a(v)\,dv$. According to Savage & Sembach (1991), this method is adequate for data with $b_{\rm line} \gtrsim 0.25 b_{\rm inst}$–$0.50 b_{\rm inst}$, where $b_{\rm line}$ is the intrinsic b-value of the line and $b_{\rm inst}$ is the b-value of the instrument. Since $b \equiv {\rm FWHM}/1.667$, for STIS E140M $b_{\rm inst} \simeq 4$ km s^{-1}, and for *FUSE* $b_{\rm inst} \approx 12$ km s^{-1}. Therefore, we assume that a negligible fraction of the gas has $b \ll 1$ km s^{-1}, an assumption made implicitly in most ISM abundance analyses using these instruments. Yet, we note that if the apparent column densities of a species with similar transitions estimated by both instruments are similar, this implies that there must be little or no unresolved saturation.

The reader should be aware that signatures of cold gas in the Bridge have been found toward DI 1388 and PKS 0312−77. The fraction of cold gas with respect to warmer gas is unknown. We note that Lehner (2002) derived $b \simeq 2.6$ km s^{-1} for the H_2 in the Bridge toward DI 1388 using a curve of growth with a single

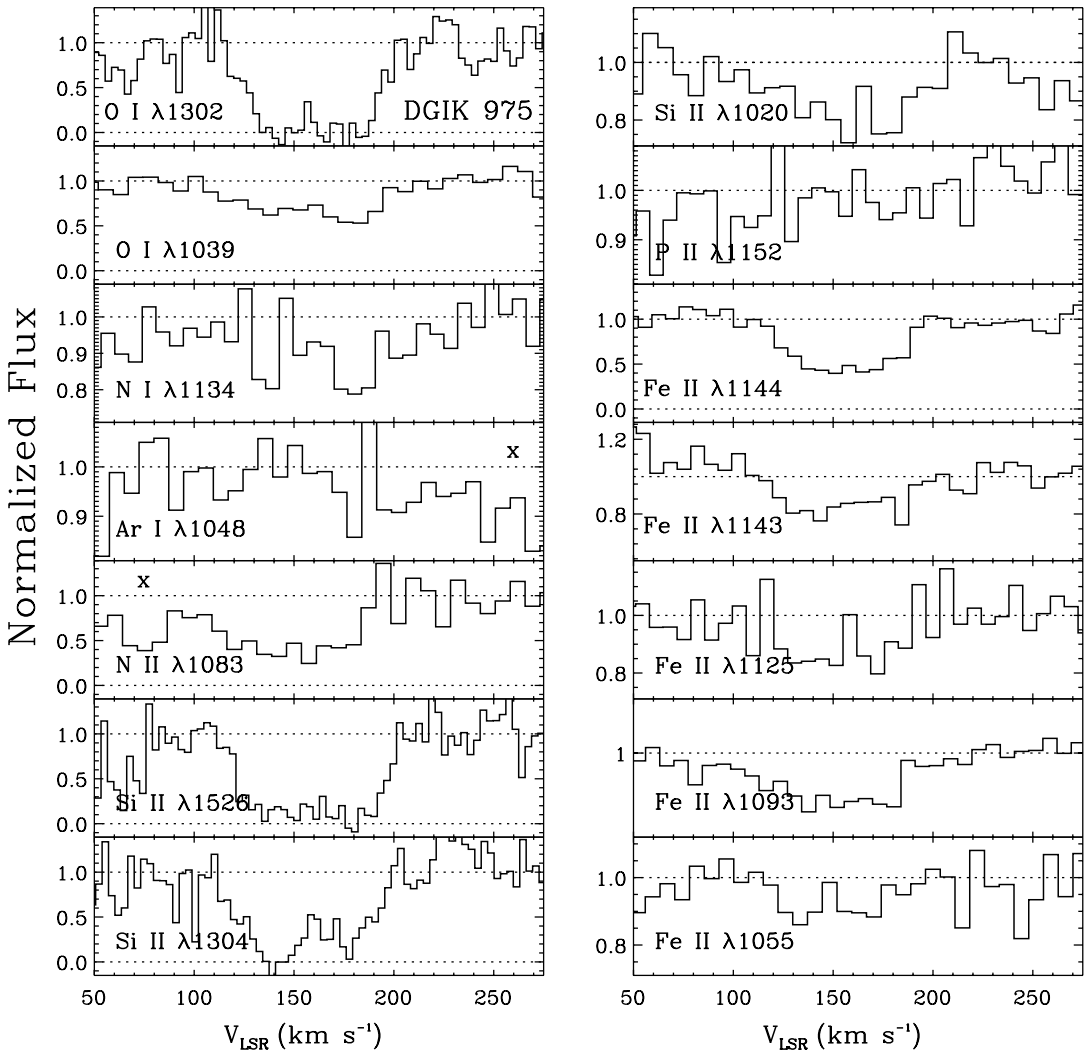

FIG. 3.—Normalized profiles against the LSR velocity near the Bridge velocities of neutral and singly ionized species in the STIS E140M and *FUSE* spectra of DGIK 975. The Bridge absorption occurs between about 100 and 200 km s^{-1} toward this line of sight. The cross shows the part of the spectrum that is contaminated by other absorbing features.

component. If a typical temperature of the molecular gas is $T \sim 100-200$ K, turbulent motions will dominate the broadening of the H_2 lines. Hence, even though there may be cold gas, turbulent motions may be important enough to keep the broadening of the atomic and ionic lines greater than 1 km s^{-1}. Because the investigated gas is multiphase (Lehner et al. 2001; Lehner 2002), the AOD method is favored over the curve-of-growth or profile-fitting methods because the AOD does not make any a priori assumptions on the kinematical distribution of the gas along the sight line. Finally, we note that our estimates are also based on nondetection of a line; these strict limits are consistent with our AOD estimates (see below), giving us confidence in the results presented here.

When $\tau_a \ll 1$ (which is the case for several transitions used in this work), unresolved saturation should not be problematic as long as b is not much smaller than 1 km s^{-1}. For stronger lines, unresolved saturated structure can be identified by comparing the lines of the same species with different $f\lambda$. Following Savage & Sembach (1991), the difference in $f\lambda$ must be a factor of 2 (or 0.3 dex) or more to be able to detect unresolved saturation. The $f\lambda$ values are summarized in Table 1. If some moderate saturation exists, we can correct for it using the procedure described in Savage & Sembach (1991). For various cases of blending and line broadening, they found a tight relation between the difference of the true column density and the apparent column density of the weaker line versus the difference of the strong-line and weak-line apparent column densities. The corrections to the apparent column density of the weak line for a given difference between the strong- and weak-line apparent column densities are summarized in their Table 4.

In cases where we only have reliable information on a single line, we only quote a lower limit on the apparent column density. However, we note that due to the low metallicity of the Bridge, the peak AODs of metal lines are generally less than 1. Even strong transitions such as O I λ1302 and N II λ1083, which have line profiles that are usually completely saturated in the diffuse gas of Galactic or SMC/LMC environments with similar H I column densities, do not reach zero flux (at least toward DI 1388).

When no absorption is observed for a given species, we measure the equivalent width (and 1 σ error) over the same velocity range found from similar species that are detected. The 3 σ upper limit on the equivalent width is defined as the 1 σ error times 3. The 3 σ upper limit on the column density is then derived assuming the absorption line lies on the linear part of the curve of growth.

In Table 1 we present our estimates of the apparent column densities for DI 1388 and DGIK 975. Below, we review each sight line separately.

TABLE 1
APPARENT COLUMN DENSITIES OF THE METALS

Species	λ (Å)	$\log f\lambda$	$\log N_a$
DI 1388			
O I	1302.168	1.795	(>)14.77 ± 0.03
O I	1039.230	0.974	(>)14.97 ± 0.06
O I	950.885	0.176	15.33 ± 0.10
O I	936.630	0.534	$15.26^{+0.13}_{-0.16}$
O I	924.950	0.154	15.32 ± 0.13
N I	1200.710	1.715	(>)14.07 ± 0.04
N I	1200.223	2.018	(>)13.89 ± 0.04
N I	1134.980	1.674	(>)14.00 ± 0.08
N I	964.626	0.882	$(\leq)14.32^{+0.13}_{-0.20}$
N I	954.104	0.582	(<)14.45
Ar I	1066.660	1.857	(<)13.17
Ar I	1048.220	2.440	12.80 ± 0.15[a]
Si II	1526.707	2.308	14.14 ± 0.07
Si II	1304.370	2.051	14.18 ± 0.02
S II	1253.805	1.136	14.25 ± 0.10
S II	1250.578	0.832	14.27 ± 0.07
Fe II	1608.451	1.970	13.95 ± 0.02
Fe II	1144.939	1.980	13.93 ± 0.05
Fe II	1143.226	1.341	13.95 ± 0.10
Fe II	1055.262	0.812	$(\leq)14.05^{+0.15}_{-0.25}$
DGIK 975			
O I	1039.230	0.974	(>)15.20 ± 0.04
N I	1134.980	1.674	$(\leq)13.88^{+0.12}_{-0.16}$
Ar I	1048.220	2.440	(<)12.92
Si II	1020.699	1.225	$(\leq)14.54^{+0.14}_{-0.20}$
Fe II	1144.939	1.980	14.18 ± 0.03
Fe II	1143.226	1.341	14.36 ± 0.07
Fe II	1125.448	1.245	14.44 ± 0.10
Fe II	1093.877	1.555	14.34 ± 0.05
Fe II	1055.262	0.812	$(\leq)14.60^{+0.10}_{-0.16}$

NOTES.—Atomic parameters are from Morton (2003). N_a is the apparent column density in cm^{-2}, except as follows: "(<)" indicates a 3 σ upper limit, "(≤)" indicates that the detection is barely 3 σ, and "(>)" indicates that the line is likely saturated (see text for more details).

[a] We note that Lehner (2002) found a column density 2 times smaller for Ar I. Lehner revisited the original reduced data (CALFUSE ver. 2.0.5) and concluded that the measurement was made using solely LiF 1A, which appears to suffer from fixed-pattern noise contamination (see Fig. 2 in Lehner 2002) but has been corrected with the new calibration. Indeed, the LiF 1A and LiF 2B segments reduced with CALFUSE ver. 3.2 give consistent results, and those are consistent with N(Ar I) determined with LiF 2B CALFUSE ver. 2.0.5 data.

DI 1388.—In Table 1 we present our raw measurements of the apparent column densities for DI 1388. Each considered species has at least two transitions with $\Delta\log(f\lambda) \gtrsim 0.3$.

Singly ionized species.—In Figure 4 we show the apparent column density profiles of Si II $\lambda\lambda$1304, 1526, and the integrated column densities agree remarkably well, especially at ~198 km s^{-1}, where the absorption is the strongest. The continuum near Si II λ1526 is somewhat more complicated than for Si II λ1304, which results in a larger uncertainty. A similar agreement is found for S II, although we note that the continuum near the blue side of S II λ1253 is more complicated. For Fe II, the data are from *FUSE* and STIS. There is again an excellent agreement between the weak and strong transitions. Furthermore, Fe II $\lambda\lambda$1608 (STIS), 1144 (*FUSE*) have similar strengths and apparent column densities. Therefore, the coarser spectral resolution of *FUSE* does not seem to affect our apparent column estimates. Hence, for the singly ionized species, there is no evidence of saturation for the lines summarized in Table 1.

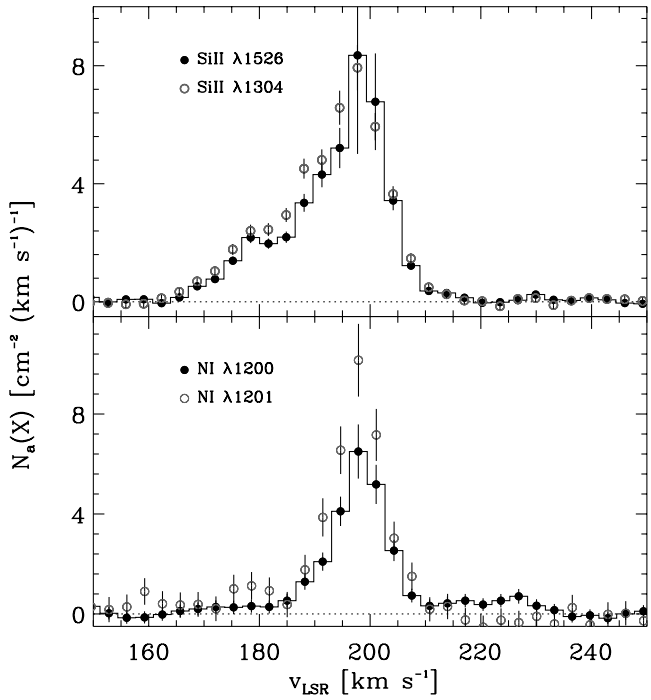

FIG. 4.—Comparison of the apparent column density profiles for Si II and N I for the DI 1388 sight line. The Si II lines are essentially fully resolved, while N I shows some unresolved saturation.

Ar I.—The transition at 1066.66 Å is a 3 σ upper limit. This is a firm upper limit irrespective of the intrinsic broadening of the line. Ar I λ1048 is detected, and its apparent column density is consistent with the weaker transition. If the strong transition has some unresolved saturation, it is likely less than 0.1 dex.

N I.—The transitions at 1200.71 and 1134.98 Å have similar strengths, but the agreement in the N_a of these two lines is not as good as for Fe II, even though the N_a estimates of these two lines overlap within 1 σ. This suggests that there may be some unresolved saturation. The apparent column density of N I λ1200.22 is 0.18 dex smaller than that of N I λ1200.711 (see also Fig. 4). Therefore, N_a(N I λ1200.711) needs to be corrected for saturation. Using the results of Savage & Sembach (1991) we find that the correction is 0.27 dex. The corrected column density of N I is therefore $\log N(\text{N I}) = 14.34 \pm 0.08$ (where the errors include statistical and saturation correction uncertainties). This result can be directly tested with the weak N I λ964 transition, a 2.8–3.1 σ detection, which yields $\log N_a = 14.32^{+0.13}_{-0.20}$ dex, in excellent agreement with our corrected column density above (note that this N I line has a strength similar to that of O I λ924 described below, but the continuum placement is much more straightforward for the O I line, explaining the difference in the errors). The upper limit on N I λ954 is also consistent with our estimate.

O I.—The strong transitions at 1302.17 and 1039.23 Å give much smaller apparent column densities than the weak lines and are therefore saturated. There are also two weak transitions at 924.95 and 950.89 Å that are 3.0–3.2 σ and 4.2–4.5 σ detections, respectively. Near the weakest transition, O I λ924, there is a contaminating feature on the blue side of the line, while there is a very weak contaminant on the red side of O I λ950 (see Fig. 2). However, the apparent column densities of O I λ924 and λ950 are consistent with each other. We also test this by measuring the half of the O I λ924 profile known to be free of contamination, and the

TABLE 2
ADOPTED COLUMN DENSITY OF THE METALS

Species	log N
DI 1388	
O I	$15.33^{+0.11}_{-0.08}$
N I	14.34 ± 0.08
Ar I	12.80 ± 0.15
Si II	14.17 ± 0.02
S II	14.26 ± 0.06
Fe II	13.95 ± 0.02
DGIK 975	
O I	>15.20
N I	$\leq 13.88^{+0.12}_{-0.16}$
Ar I	<12.92
Si II	$\leq 14.54^{+0.14}_{-0.20}$
Fe II	$14.38^{+0.12}_{-0.05}$

NOTE.—See § 3.1 for more details.

resulting $N_a \times 2$ is consistent with the value reported in Table 1. The continua near these lines are well modeled with a straight line. O I $\lambda\lambda$924, 950 have $\tau_a \ll 1$ and similar $f\lambda$. O I λ936 is about 0.3 dex stronger than these lines and can be used to test for any unresolved structures. However, this line is partially blended with H I λ937, complicating the continuum placement, which results in a larger error. Within the errors, the apparent column densities of the three lines are consistent. Nevertheless, to be cautious, we adopt the weighted average of the apparent column densities of O I $\lambda\lambda$924, 950 and add an error in quadrature of +0.07 dex to include any possible weak saturation. Our adopted O I column density is $\log N(\mathrm{O\ I}) = 15.33^{+0.11}_{-0.08}$.

DGIK 975.—The STIS data are of lower quality than those for DI 1388, and the peak AODs are greater than 1 for all the detected species (see Fig. 3). We therefore use only the *FUSE* data. Unfortunately, the *FUSE* stellar spectrum is not as well behaved as that of DI 1388, and we often have to rely on a single line. Stellar contamination and the amount of H I are more important (see § 3.2), so that none of the weak O I and N I lines can be used. The λ1039 transition is the only available O I line and is likely saturated, providing a firm lower limit. (The apparent column density of O I λ1302 cannot be estimated because the signal-to-noise ratio is too low and its absorption reaches zero flux.) Ar I λ1048 is not detected and provides a firm 3 σ upper limit. N I λ1134 is a 2.8–3.2 σ detection, and therefore the estimate of the apparent column should be considered as an upper limit. The same applies for Si II λ1020 (the measurement of this line being complicated by the uncertain continuum placement). Only for Fe II can several transitions be measured. Following the above method, we estimate the average column density using the weak lines (i.e., excluding Fe II λ1144) and add a systematic error to take into account possible unresolved structures.

Our adopted column densities for neutral and singly ionized species are summarized in Table 2. There is an overall agreement with previous column density estimates (Lehner et al. 2001; Lehner 2002); in particular, if in Lehner (2002) the O I and N I column densities estimated in the DI 1388 spectrum are systematically smaller than currently, they nonetheless overlap within 1.5 σ. The main difference is that he relies on a single-component curve-of-growth analysis using both weak and strong lines, which depends on an assumed velocity distribution that is likely more complex than one Gaussian component. We believe using the AOD method is a better approach to determine the most reliable column densities and errors in view of the complexity of the velocity distribution in these sight lines.

3.2. *Neutral Hydrogen*

Here we discuss our derivation of the Bridge H I column based on the analysis of the Lyα absorption. The H I column density is more complicated to derive because both the Galaxy and Bridge contribute to the absorption. H I 21 cm emission observations toward the stars are of little use for the Bridge component because the stars are embedded in the Bridge with an unknown depth. We therefore need to derive N(H I) from the Lyα absorption. To do so, we fit each damped Lyα absorption-line profile with two components that correspond to the Galactic and Bridge components. The blueward wing of the profile is due primarily to the Galactic component, but the Galactic component cannot completely account for the absorption in the redward wing, indicating the need for a Bridge component. By fixing the velocities of the Galactic and Bridge components, we can determine the H I column densities. We note that the amount of H I gas between the Galaxy and the Bridge is negligible, since the H I 21 cm data do not show any emission toward these two lines of sight at a level of $10^{18.3}$ cm^{-2}, too small to affect the damping wings of Lyα. O I is the best metal proxy for H I, since its ionization potential and charge exchange reactions with hydrogen ensure that the ionization of H I and O I are strongly coupled. We can therefore use the kinematics of O I to infer those for H I. While the O I profiles show multiple structures in both the Galactic and Bridge components, we only use the average velocities to fix the values for each component. These are listed in Table 3. Below, we detail our fitting results for each star.

TABLE 3
H I COLUMN DENSITY

Sight Line/Component	v_{LSR} (km s^{-1})	log N	log $N^\star$	log N_{adopted}
DI 1388 MW	−5	20.41 ± 0.02	...	20.41 ± 0.02
DI 1388 Bridge	195	19.67 ± 0.07	18.58	19.63 ± 0.07
DGIK 975 MW	−5	20.95 ± 0.08	...	20.95 ± 0.08
DGIK 975 Bridge	160	19.95 ± 0.30	18.98	19.90 ± 0.30
PKS 0312−77 MW	5	20.78 ± 0.06	...	20.78 ± 0.06
PKS 0312−77 Bridge	210	20.12 ± 0.30	...	20.12 ± 0.30

NOTES.—The LSR velocities are fixed and estimated from the O I absorption profiles. N is the observed column density, $N^\star$ is the estimated stellar H I contribution for the Hβ profiles (see text for more details), and N_{adopted} is corrected for the stellar component in the Bridge component. Note that the errors include different choices of continuum placement and polynomial degree for the continuum and velocity shifts of ± 5 km s^{-1}.

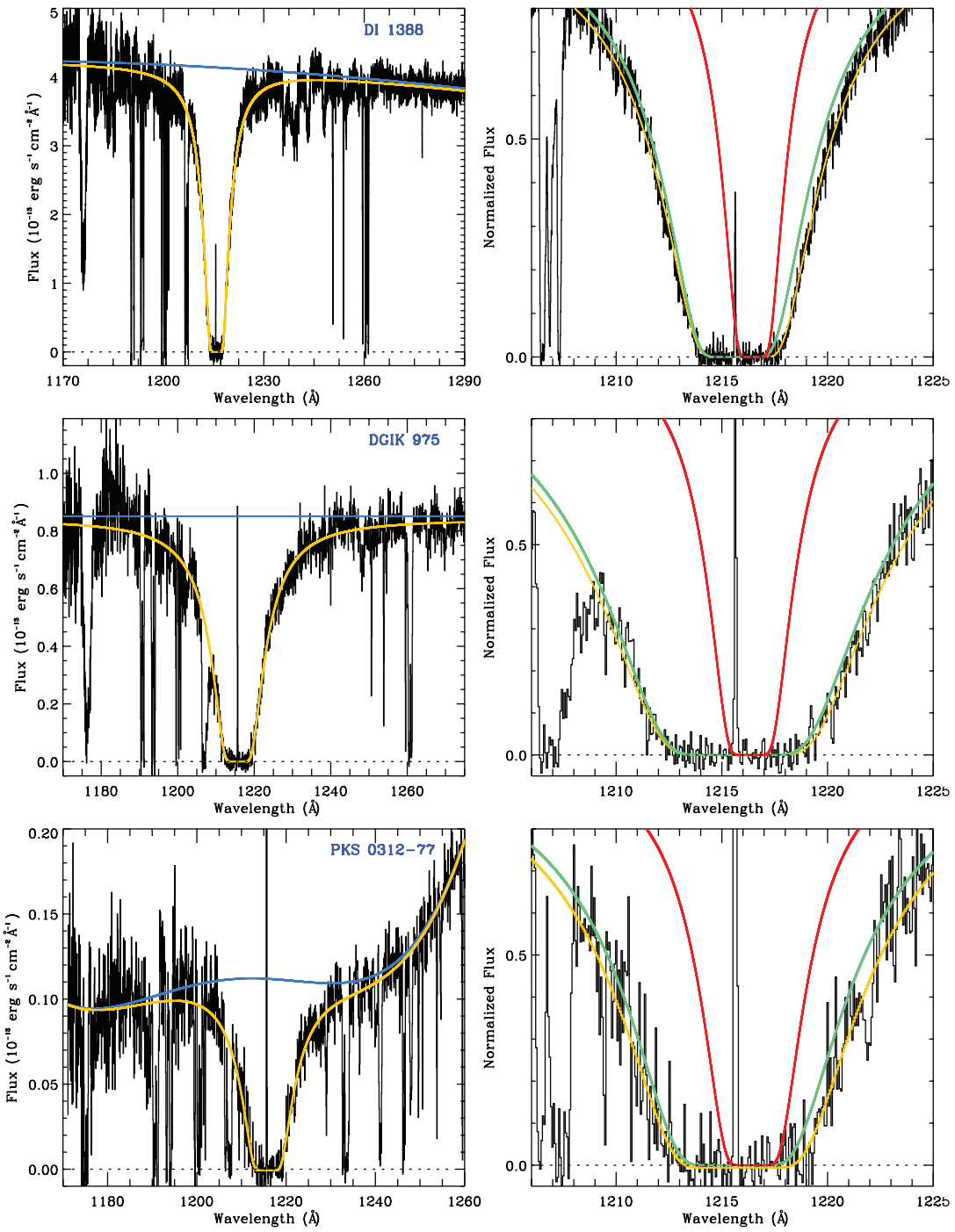

FIG. 5.—*Left panels*: Lyα profiles in the STIS E140M spectra of DI 1388 (*top*), DGIK 975 (*middle*), and PKS 0312−77 (*bottom*). The blue line shows the continuum, and the yellow line shows the two-component fit to the interstellar Lyα profile. *Right panels*: Zoom-in on the core of the normalized Lyα profiles for each line of sight. The yellow line shows the two-component fit, while the green and red lines show only the Galactic and Bridge components, respectively.

DI 1388.—This line of sight is our best case because the continuum of the star is well behaved and the Galactic H I column density is not so large that it fills the absorption in the red part of the Lyα profile to a large degree. In Figure 5 we show the profile of Lyα with its continuum and the fit with the two components (*top left panel*). In the top right panel we show part of the normalized Lyα profile with the two-component fit (*yellow line*), the Bridge component (*red line*), and the Milky Way component (*green line*). This shows that while the Galactic component nearly fits the blue part of the Lyα absorption, there is extra absorption in the red part that is missed by the Galactic component. In the third column of Table 3, we summarize the derived column density for each component. To test the robustness of our fit, we undertook many simulations where the velocity centroids were changed by ± 5 km s^{-1}, the placement of the continuum was varied, and the continuum was modeled by a range of polynomials of first to fourth degree. The errors reported in Table 3 are estimated to reflect the 1 σ distribution between all the trials.

DGIK 975.—This line of sight is more complicated because the Galactic H I component is much stronger than that toward DI1388. For the latter, the Galactic H I component is about a factor of 5 stronger than the Bridge component, while toward DGIK

975 we found that the Galactic component is ~10 times stronger than that of the Bridge. The Si III λ1206 line is also very strong and removes some information in the blue part of the Lyα absorption. Finally, the STIS E140M DGIK 975 spectrum has a much lower signal-to-noise ratio; we therefore rebinned these data by 5 pixels before fitting. In Figure 5 we show our resulting best fit overplotted on the Lyα profile (*middle left panel*), where the continuum is well behaved and can be modeled by a straight line. The normalized profile (*middle right panel*) indeed shows that the difference between the two-component fit and the single Galactic component fit is small, which results in a large error in the N(H I) of the Bridge feature. However, as for DI 1388, at 1219 Å $\lesssim \lambda \lesssim$ 1222 Å, where the optical depth is more important, the Galactic component does not properly fit the red part of the absorption without the Bridge component. We also undertook several trials in order to derive the 1 σ error reported in Table 3.

The H I 21 cm emission data can help evaluate the solution from our fits, at least for the Galactic component; indeed, since the whole column of Galactic gas is probed in both emission and absorption toward the stars, the inferred column densities derived from absorption and emission spectra can be compared. The main uncertainty that arises from such a comparison is that the beam that collected the H I 21 cm emission data is much larger than the pencil-like beam of the absorption observations. Therefore, the beam of the radio telescope only represents an average column density of the region near the line of sight. Wakker et al. (2001) studied this effect for low-, intermediate-, and high-velocity clouds (HVCs) by comparing N(H I) measured via beams of 36′, 9′, and 1′ and through Lyα absorption. They found that the "beam effect" was less important for the low-velocity gas where the range of the ratio of N(H I) measured with a 9′ beam versus a 36′ beam is 0.9–1.4 than for the HVCs where the range of the ratio is 0.3–2.1. This difference occurs because the physical sizes probed by the H I 21 cm data are naturally smaller in nearby gas and therefore less likely to have large angular/spatial variations. Hence, H I 21 cm emission observed through a 15′ beam should provide reliable N(H I) within a beam error of about ±0.10 dex (see also Lehner et al. 2004) for the low-velocity Galactic gas that can be compared to the results from the profile fitting of the Lyα absorption.

With H I 21 cm emission observations from the Parkes 64 m radio telescope with a 15′ beam and 1 km s^{-1} spectral resolution (M. E. Putman 1999, private communication) we derive the H I column density for the Galactic component, where we make the usual assumption that the medium is optically thin: $\log N(\mathrm{H\ I}) = 20.44 \pm 0.11$ toward DI 1388 and $\log N(\mathrm{H\ I}) = 20.85 \pm 0.11$ toward DGIK 975. Using the 21 cm emission data from the 36′ Leiden-Argentine-Bonn survey (LAB) within ~1° of the star's coordinates (Kalberla et al. 2005; Bajaja et al. 2005), we find Galactic H I column densities that are systematically similar to those quoted above within the errors. Within 1 σ, the H I column densities of the Galactic component derived from emission and absorption observations are consistent.

Finally, we also consider the QSO PKS 0312−77 sight line. Since both the UV and radio observations probe the full depth of the Bridge, we can compare the resulting H I column densities measured with both observations with the caveat that we have to assume that small-scale variations in the 15′ beam (corresponding to about 240 pc at 55 kpc) are small enough in the direction of PKS 0312−77. Kobulnicky & Dickey (1999) detected H I 21 cm emission for the Bridge component with the Parkes telescope toward this line of sight. They derived a Bridge H I column density of $\log N(\mathrm{H\ I}) = 20.09 \pm 0.13$, where the errors include the statistical error and systematics associated with the beam that is larger than our pencil beam for the UV observations (see above). We note that the LAB data give systematically larger N(H I) for the Bridge but with relatively small variations within a radius (in the l, b plane) of ~40′; the closest LAB pointing is 4′ away, where $\log N(\mathrm{H\ I}) = 20.23 \pm 0.25$ and the range of $\log N$(H I) is between 20.18 and 20.34 dex [toward the two stars, the variation in N(H I) is quite large, a factor of 2–3, within the same radius].

The Lyα profile of PKS 0312−77 is shown in Figure 5 (*bottom left panel*) and is clearly more challenging to model than those for the two stars, as the signal-to-noise ratio is lower (the data shown were rebinned by 5 pixels) and the red part of the continuum is heavily affected by emission lines from the QSO (emission from Lyβ, O VI, and O I), complicating the continuum placement. The Galactic component is also strong, but because all of the Bridge gas is probed along this line of sight, this results in a higher H I Bridge column density than toward the two stars. In Figure 5 we show one of our best fits, and, as for the other lines of sight, the errors reflect many trials. However, because of the complexity of the continuum, the degree of the polynomial was allowed to vary between 2 and 7; a fifth-degree polynomial is shown in the figure. The Galactic component again cannot account for absorption at $\lambda \gtrsim 1219$ Å. Table 3 summarizes the results, and, while the error is large, the measured value of $\log N(\mathrm{H\ I}) = 20.12 \pm 0.30$ is quite consistent with the H I 21 cm column density derived by Kobulnicky & Dickey (1999). These authors do not provide N(H I) for the Galactic component, but using the LAB data we estimate that it is $\log N(\mathrm{H\ I}) = 20.83 \pm 0.17$, consistent with the Ly$\alpha$ absorption estimate in the Galactic component.

The general agreement between the N(H I) estimates from absorption and emission measurements gives further confidence in our fits to the Lyα absorption observed along each line of sight. The error estimates were systematically estimated via several fit trials, and we believe that we are conservative in our error estimates. However, the stellar sight lines need to be corrected for contributions from the stellar photospheres. We follow the method originally presented by Diplas & Savage (1991) and expanded by Howk et al. (1999) to estimate the stellar Lyα contribution, which involves measuring the photospheric Hβ equivalent width of each star and using equation (A7) in Howk et al. to estimate W(Lyα). The stellar H I column density is then derived via $\log N(\mathrm{H\ I}) = 18.27 + W(\mathrm{Ly}\alpha)$. Using our AAT spectra, we estimate that $W(\mathrm{H}\beta) = 2.1 \pm 0.2$ Å for DGIK 975 and $W(\mathrm{H}\beta) = 2.1 \pm 0.2$ Å for DI 1388. This corresponds to stellar H I logarithm column densities of 18.58 and 18.98 for DI 1388 and DGIK 975, respectively. The correction is larger for DGIK 975 because the temperature of the star is lower than the temperature of DI 1388. The last column of Table 3 reports the Bridge H I column densities corrected for the stellar contribution.

4. ABUNDANCES AND PHYSICAL CONDITIONS IN THE MAGELLANIC BRIDGE

4.1. *Metallicity*

In Figure 6 we show the ratio of the apparent column densities of O I and N I to N_a(S II) normalized to the solar abundances for the DI 1388 sight line. Sulfur is our reference because it is not depleted into dust. Also note that throughout the text we use the following notation: $[X^i/Y^j] = \log N(X^i)/N(Y^j) - \log (X/Y)_\odot$, and we adopt the solar abundances of Asplund et al. (2006).[4] We

[4] For the species used throughout this work, the following are the adopted solar abundances $\log (X/\mathrm{H})$: C, -3.61 ± 0.05; N, -4.22 ± 0.06; O, -3.34 ± 0.05; Si, -4.49 ± 0.02; Ar, -5.82 ± 0.08; S, -4.85 ± 0.03; and Fe, -4.55 ± 0.03 (Asplund et al. 2006). Note that our error estimates do not take into account the solar abundance errors.

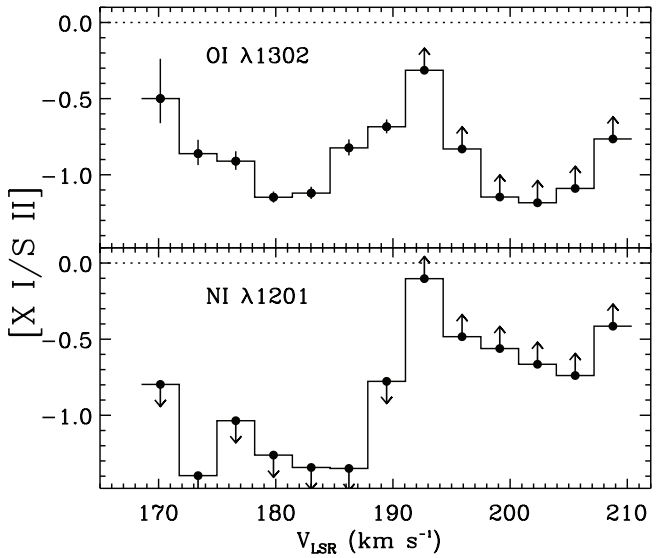

FIG. 6.—Relative gas-phase abundance of O I and N I with respect to S II (where λ1250) for the DI 1388 sight line. At $v_{\rm LSR} \gtrsim 193$ km s^{-1}, O I and N I absorption suffers from saturation.

TABLE 4
GAS-PHASE ABUNDANCES OF THE BRIDGE

Species	$[X/{\rm H}]$
DI 1388	
N I	-1.07 ± 0.11
O I	$-0.96^{+0.13}_{-0.11}$
Ar I	$-1.01^{+0.16}_{-0.17}$
DGIK 975	
N I	$(\le) -1.75^{+0.31}_{-0.38}$
O I	$>-1.36 \pm 0.30$
Ar I	$<-1.16 \pm 0.30$

NOTES.—The adopted solar abundances are from Asplund et al. (2006): N, −4.22; O, −3.34; and Ar, −5.82. The uncertainties in the solar abundances are not taken into account in the errors listed in the table. A "<" sign means a 3 σ upper limit.

explicitly retain the ionization state information to emphasize the impact of ionized gas on these measurements. As already discussed by Lehner et al. (2001), the Bridge gas toward DI 1388 has two main components, one mostly ionized (165 km s^{-1} $\le v_{\rm LSR} \le$ 193 km s^{-1}) and the other partially ionized (193 km s^{-1} $< v_{\rm LSR} \le$ 215 km s^{-1}). The extremely ionized gas is illustrated by [O I/S II] $\simeq -1$ for 170 km s^{-1} $\le v_{\rm LSR} \le$ 193 km s^{-1} (S II is important in both neutral and ionized gas, but O I arises only in neutral gas). Toward DGIK 975, the normalized profiles shown in Figure 3 suggest a similar pattern: two main components are observed, and the higher velocity component is more neutral than the lower velocity component, as revealed by the stronger absorption in O I and N I and weaker Fe II at 175 km; the opposite pattern is observed at 140 km s^{-1}. Therefore, singly ionized species cannot be directly used to estimate the metallicity of the gas because they contain a significant contribution from ionized gas.

On the other hand, the ionization of oxygen and hydrogen are strongly coupled, and oxygen is only mildly depleted into dust grains (up to −0.16 dex using the updated O I abundance [see below]; Meyer et al. 1998), implying that the O I/H I ratio is the best indicator of the metallicity of the Bridge gas. We note that both the H I column densities and molecular fraction in Meyer et al. (1998) are typically much larger than those in the Bridge gas. The oxygen measurements in the Local Bubble imply a depletion of −0.12 dex (Oliveira et al. 2005). Therefore, the depletion of O in the Bridge is likely to be less than −0.1 dex. We find that the Bridge gas oxygen abundance is [O I/H I] $= -0.96^{+0.13}_{-0.11}$ toward DI 1388. Toward DGIK 975, only a lower limit is derived (see Table 4). We note that the solar abundance of O has changed quite significantly over the years, and the new value may still be controversial. Prior measurements of Asplund et al. (2006) gave a solar O abundance +0.17 dex larger (Grevesse & Sauval 1998); i.e., the Bridge O abundance would be further below.

The solar Ar and N abundances appear more settled, with little change between those listed in Grevesse & Sauval (1998) and Asplund et al. (2006). Furthermore, Ar and N are not depleted into dust grains (Sofia & Jenkins 1998; Meyer et al. 1997), and Ar I and N I behave like O I in gas with large H I column density (see Fig. 6 in Lehner et al. 2003); i.e., the ionization fractions of these elements are coupled with the ionization fraction of H via a resonant charge-exchange reaction. Toward DI 1388, the values of the N and Ar abundances summarized in Table 4 show excellent agreement with those of O. This might appear puzzling at first glance, since O I is clearly detected in both components, while Ar I and N I absorption is mostly absent in the 180 km s^{-1} component. However, the neutral gas is clearly dominated by the component at 198 km s^{-1}, since the column density in the 180 km s^{-1} component is only about 10% of the total O I column density [where we estimate $\log N({\rm O\ I}) \simeq 14.22$ in the 180 km s^{-1} component from a profile fit to the O I $\lambda\lambda$1302, 1039, 963 lines].

The AOD estimate of S II for 193 km s^{-1} $\le v_{\rm LSR} \le$ 215 km s^{-1} is $\log N({\rm S\ II}) = 13.98 \pm 0.08$. Assuming that 90% of the observed H I is in this component (based on O I) yields [S II/H I] $\simeq -0.8$. Since absorption of C III, N II, and Si III is found in this velocity range, this component is partially ionized. Therefore, the [S II/H I] provides a strict upper limit to the abundance of S, since the gas is partially ionized in this component.

We mentioned above that O could be slightly depleted into dust. If we assume an oxygen depletion of 0.05 dex (which is still consistent with the S abundance in the Bridge and about 25% ionized gas in this component), [Ar I/O I] ~ -0.1 and [N I/O I] ~ -0.2. In low-metallicity gas, N is generally found deficient (e.g., Henry & Prochaska 2007; although we note for a metallicity of −1 dex that [N/O] is more typically −0.5 dex), and this could explain the lower abundance of N. Nucleosynthesis history is unlikely to affect the Ar/O ratio, since they are both α-elements. But Ar I may be deficient because of photoionization (see Fig. 6 in Lehner et al. 2003), although with $\log N({\rm H\ I}) = 19.6$ one would likely expect a deficiency less than 0.1 dex (except possibly if a hard-ionization source overionizes the edge of the neutral gas). (The Grevesse & Sauval [1998] value gives a large O depletion, but the [N I/O I] would be less deficient.) The errors can accommodate a slight O depletion (as compared with Ar and N) or none; we therefore use a weighted average of the abundances of O I, N I, and Ar I to derive the metallicity of the gas within the Bridge: $[Z/{\rm H}] = -1.02 \pm 0.07$.

Although the errors are large toward DGIK 975, the limits on Ar I and N I suggest an extremely low metallicity as well. Using Ar I and O I (both α-elements), we can bracket the metallicity of the Bridge gas toward DGIK 975: $-1.7 < [Z/{\rm H}] < -0.9$. We note that toward this sight line N may appear more deficient than the α-elements.

Our gas-phase metallicity is in agreement with the metallicity derived from three Bridge B-type stars, where the average is -1.1 ± 0.1 dex (Rolleston et al. 1999; Lee et al. 2005). Since the interstellar and stellar abundance measurements are made using different techniques and have different systematics, the present-day metallicity of the Bridge is now secure, with an average value $[Z/H] = -1.05 \pm 0.06$ dex. This is about a factor of 3 times smaller than the SMC abundance of -0.6 dex solar (see, e.g., Welty et al. 1997; Russel & Dopita 1992; and references therein). In § 5 we discuss the implication of the metallicity results.

4.2. *Ionization and Molecular Fraction*

Using the measurement of H I along our two stellar sight lines, one can estimate the fractions of neutral, ionized, and molecular gas. Assuming an average Bridge metallicity from the stellar and interstellar measurements of about -1 dex solar, we can use the singly and doubly ionized species to estimate the amount of ionized gas. Toward DI 1388 we use sulfur, since this element is not depleted into dust and has the same nucleosynthetic history as O and Ar (because these are all α-elements). Using the total column densities listed in Table 1, we find that the total hydrogen column density ($H = H\,I + H\,II + H_2$) is

$$\log N(\mathrm{H}) = \log[N(\mathrm{S\ I}) + N(\mathrm{S\ II}) + N(\mathrm{S\ III})] - \log(Z_{\mathrm{MB}}/Z_{\odot}) - \log(\mathrm{S/H}_{\odot}) \simeq 20.2 \text{ dex},$$

where we estimate $\log N(\mathrm{S\ III}) = 13.63^{+0.11}_{-0.15}$ from the line at 1012.495 Å using the AOD method and N(S I) is negligible. Lehner (2002) derived $\log N(H_2) = 15.45$ toward DI 1388. The fraction of neutral gas is therefore $f(\mathrm{H\ I}) = N(\mathrm{H\ I})/N(\mathrm{H}) = 0.27$, while the fraction of molecular gas is $f(H_2) = 2N(H_2)/N(\mathrm{H}) = 3.6 \times 10^{-5}$. Therefore, about 70% of the gas toward DI 1388 is ionized. As we discussed above, the lower velocity Bridge gas is nearly fully ionized (∼95%), while the higher velocity Bridge gas is partially ionized (∼53%, assuming the O abundance from Asplund et al. [2006] and that O is not depleted into dust).

The near absence of N I and Ar I in the low-velocity gas of the Bridge toward DI 1388 can be mostly explained by photoionization. Indeed, if steady photoionization dominates, Ar I is deficient because the photoionization cross section of Ar is about 10 times that of H over a broad range of energy. In our Galaxy, Ar I has been found to be deficient with respect to O I (Sofia & Jenkins 1998; Jenkins et al. 2000; Lehner et al. 2003). In partially ionized gas, N also behaves more like Ar than O (Jenkins et al. 2000; Lehner et al. 2003). Ionization is unlikely to affect the higher velocity gas because the N(H I) is large enough to shield the gas against ionizing photons. Since there are hot early-type stars in the Bridge, a potential source for ionization is photoionization by these objects. In § 5.1 we discuss further the possible sources of ionization. We also note that nucleosynthesis may also lower the N abundance. Using the lower limit on N II (>14.19 dex) and the H column density derived above, $[\mathrm{N/H}] > -1.51$ (N III is negligible; see Lehner 2002). It is therefore not clear whether N is deficient or not, although it appears less deficient than usually observed for gas with a metallicity of 0.09 solar (Henry & Prochaska 2007 and references therein).

Using the same arguments as above for DGIK 975 (and assuming a metallicity of -1 dex), but employing Fe II and Fe III [where we estimate $\log N(\mathrm{Fe\ III}) = 14.29 \pm 0.06$ from the line at 1122.524 Å and assume that Fe III is not contaminated by the star] and correcting for the depletion of Fe (where we assume it is -0.6 dex based on the similarity of the [Fe II/Si II] toward both stellar sight lines and that the same depletion applies for Fe II and Fe III), we find $\log N(\mathrm{H}) \sim 20.8$, which implies that ∼75%–95% of the gas is also ionized along this line of sight. No H_2 has been found toward this sight line, implying $f[H_2] \lesssim 5 \times 10^{-6}$. As for DI 1388, the low-velocity component appears more ionized than the higher velocity cloud (see above), but the Bridge gas toward DGIK 975 appears even more ionized than that along the DI 1388 sight line.

Toward PKS 0312−77, we estimate via the AOD method $\log N(\mathrm{S\ II}) = 14.95 \pm 0.07$ using the S II $\lambda\lambda$1250, 1253 lines. From the H I column density derived by Kobulnicky & Dickey (1999), we find that $[\mathrm{S\ II/H\ I}] = -0.29 \pm 0.16$. Assuming that the metallicity is -1 dex along this sight line, this implies again that about 70%–85% of the gas is ionized toward PKS 0312−77. We note that this line of sight probes the whole depth of the Bridge and therefore shows that ionized gas appears significant everywhere. We also note that none of these estimates take into account the highly ionized phase probed by O VI, Si IV, and C IV absorption (see Lehner et al. 2001; Lehner 2002). The weakly and highly ionized gases are unlikely to probe the same material; therefore, these ionized fractions should be considered as lower limits.

4.3. C II* *Diagnostic*

C II* can be used to estimate the electron density and radiative cooling rate of the gas (see, e.g., Lehner et al. 2004). In ionized gas and cold neutral gas, C II radiation is a far more important coolant than in warm neutral gas (Wolfire et al. 1995). Toward DI 1388, C II* is detected between 193 and 215 km s^{-1}, i.e., in the partially ionized component, but it is absent between 165 and 193 km s^{-1}, i.e., in the nearly fully ionized component (see Fig. 7). We find $\log N(\mathrm{C\ II^*}) = 12.77 \pm 0.11$ with an average velocity of $v_{\mathrm{LSR}} = 202.8 \pm 1.5$ km s^{-1} and a b-value of $b = 4.2 \pm 1.1$ km s^{-1} (obtained from a single-component profile fit), which implies $T < 2 \times 10^4$ K. It is therefore not clear whether C II* arises in some ionized gas at $T \sim 10^4$ K or in cold neutral gas where turbulent motion may be important. For the gas observed at 165 km s^{-1} $\leq v_{\mathrm{LSR}} \leq$ 193 km s^{-1}, we derive a 3 σ upper limit: $\log N(\mathrm{C\ II^*}) < 12.18$. Toward DGIK 975, the 3 σ upper limit is 13.4 and is not useful.

If we assume that the electron collisions dominate the excitation of C II, the electron density within the Bridge can be written as (see Lehner et al. 2004)

$$n_e \simeq 0.183\sqrt{T}\frac{N(\mathrm{C^{+*}})}{N(\mathrm{C^+})}\ \mathrm{cm^{-3}}. \quad (1)$$

We assume a temperature of $T \sim 10^4$ K (typically observed in ionized gas; e.g., Howk et al. 2006). We use S II as a proxy of C II and assume that carbon is 0.25 dex depleted (Cardelli et al. 1996 and using the updated Asplund et al. 2006 solar C abundance). For gas at 165 km s^{-1} $\leq v_{\mathrm{LSR}} \leq$ 193 km s^{-1}, we find $\log N(\mathrm{S\ II}) = 13.94 \pm 0.08$, and therefore $n_e < 0.03$ cm^{-3} (3 σ) at $T = 10^4$ K. Since this gas is nearly fully ionized, $n_e \approx n_p$, and therefore the overall density of the ionized gas is quite low. From S II, $\log N(\mathrm{H}) \sim 19.8$ (including S III would increase this column by at most 0.2 dex); the path length of probed ionized gas is >0.6 kpc. Since the projected size of the Bridge is about 5 kpc, DI 1388 is likely not deeply embedded in the Bridge (this is consistent with the comparison of the column densities from H I emission and H I absorption). For the gas at 193 km s^{-1} $\leq v_{\mathrm{LSR}} \leq$ 215 km s^{-1}, we find $n_e < 0.1$ cm^{-3} at $T = 10^4$ K (here it is an upper limit because the C II* absorption could possibly arise in cold gas).

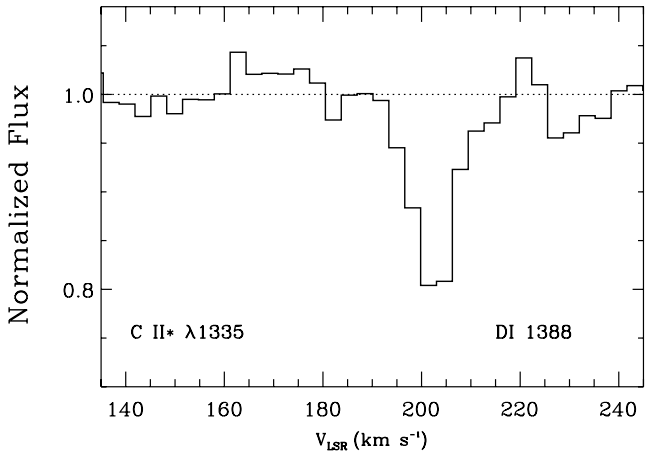

FIG. 7.—Normalized profile of C II* against the LSR velocity. Note the absence of absorption between ~160 and 190 km s^{-1} where the nearly fully ionized component is observed.

TABLE 5

SUMMARY OF THE PROPERTIES IN THE DIFFUSE GAS OF THE BRIDGE

Parameter	Value
$[Z/H]$[a]	-1.05 ± 0.06
[O VI/H]	-3.8 to -3.3
[O VI/H I]	-3.1 to -2.3
Depletion of Si	-0.45 ± 0.06
Depletion of Fe	-0.61 ± 0.06
Fraction of total H I	~20%
Fraction of total H II	~80%
Fraction of H_2	$\lesssim 0.004\%$
Density $n_e \simeq n_p$[b]	$<0.03-0.1\sqrt{T_4}$ cm^{-3}
Total H mass[c]	$\sim 9 \times 10^8\ M_\odot$

[a] Average metallicity from the interstellar and B-type stellar estimates.

[b] Density of ionized gas. T_4 is the temperature in units of 10^4 K.

[c] Adopting a total H I mass of $1.8 \times 10^8\ M_\odot$ (Brüns et al. 2005) and assuming that the fraction ionized is 80% throughout the Bridge. Note that the *total* mass of the Bridge should include the H+He mass.

Since the Hα intensity scales with the square of the density, it is not surprising that most of the current Hα observations of the Bridge outside dense H II regions yield no Hα detection down to $I[\mathrm{H}\alpha] < 0.5$–2 R (Putman et al. 2003; Muller & Parker 2007). For the Galactic warm ionized medium (WIM), Lehner et al. (2004) estimated the relationship between C II* produced in the WIM and the intensity of Hα. Adapting their relationship (eq. [7] in their paper) to the Bridge conditions, $I[\mathrm{H}\alpha] \simeq 1.5 \times 10^{-13} N_{\mathrm{WIM}}(\mathrm{C\ II}^*)$ R [where $N_{\mathrm{WIM}}(\mathrm{C\ II}^*)$ is in cm^{-2}]. With our 3 σ upper limit $\log N(\mathrm{C\ II}^*) < 12.18$, we derive $I[\mathrm{H}\alpha] < 0.2$ R, typically smaller than the current limits from Hα observations. In the partially ionized component, $I[\mathrm{H}\alpha] < 0.9$ R. Future deep Hα observations with the Wisconsin Hα Mapper (WHAM) currently being installed in Australia should yield important clues to the faint, diffuse Hα emission in the Bridge and other tidal structures around the Magellanic Clouds.

The C II radiative cooling rate is expressed as (see Lehner et al. 2004)

$$l_c = 2.89 \times 10^{-20} \frac{N(\mathrm{C}^{+*})}{N(\mathrm{H})}\ \mathrm{erg\ s^{-1}\ (H)^{-1}}. \qquad (2)$$

As discussed, the C II* absorption is only detected in the partially ionized gas. Most of the H I is contained in this component, and therefore the C II radiative cooling rate is 4.5×10^{-27} erg s^{-1} (H I)$^{-1}$. We can express this as the cooling per nucleon if we use the amount of S II present in this component; we derive $l_c < 2.8 \times 10^{-27}$ erg s^{-1} (H)$^{-1}$ (it is an upper limit because we neglected S III). Since the cooling rate is directly proportional to the metallicity of the gas for the ionized material (e.g., Wolfire et al. 2003), these cooling rates per metal are similar to the Galactic average rate within the 1 σ dispersion derived by Lehner et al. (2004) at similar N(H I) or N(H). Where we do not detect C II*, $l_c < 7 \times 10^{-28}$ erg s^{-1} (H)$^{-1}$, much smaller than those observed in the Milky Way at low N(H I).

5. DISCUSSION

In Table 5 we summarize the properties of the Bridge derived from this work. The most recent estimate of the H I mass of the Bridge was derived by Brüns et al. (2005), and to estimate the H mass of the Bridge we assume that the large ionization fraction in the Bridge observed in our three lines of sight is characteristic of the Bridge as a whole. Since our sight lines probe very different regions of the Bridge, the hypothesis that the ionization fraction is large in most regions of the Bridge appears reasonable. This mass is ~5 times larger than usually estimated in current models (e.g., Muller & Bekki 2007). However, since the gas mass fraction of the SMC and LMC and the ratio of the gas disk to the stellar disk of the SMC can be adjusted in models, and since the SMC mass is not known to better than a factor of 2, it is possible that simulations may be able to accommodate a larger Bridge mass.

5.1. *Sources of Ionization of the Bridge*

One likely source of ionization of the Bridge is the stars within it. A young population of stars was discovered throughout the Bridge (Irwin et al. 1990; Bica & Schmitt 1995; Demers & Battinelli 1998). The density of OB associations is, however, not uniform; the OB-type stars are highly concentrated in the SMC Wing where the H I column densities are largest (roughly delimited by the box in Fig. 1) and are far more sparse farther away from the SMC (Irwin et al. 1990; Battinelli & Demers 1992). The box in Figure 1 also corresponds to the CO survey undertaken by Mizuno et al. (2006) where CO emission was discovered, suggesting that conditions might be conducive to star formation. We note that the star formation history must be quite different from the less dense region of the Bridge (see § 5.3), since in the SMC Wing, an SMC-like metallicity is derived from the analysis of B-type stars (Lee et al. 2005).[5] Yet, the presence of early-type stars 20 Myr old or younger well inside and throughout the Bridge (Demers & Battinelli 1998; Rolleston et al. 1999) implies ongoing star formation at some level.

[5] There might be some confusion in the literature with the nomenclature "SMC Wing" and "Bridge" (also called the intercloud region). In some cases, the Wing is an environment by itself (usually in studies of stars); in other cases (usually in studies of CO and H I emission) it is a direct component of the Bridge. The latter is possible and seems to be justified in view of the H I column density and velocity maps. But the SMC Wing has a much higher concentration of OB associations (Irwin et al. 1990) and an SMC-like metallicity (Lee et al. 2005), which seem to imply a different evolution from the Bridge at R.A. (J2000.0) $\gtrsim 2^{\mathrm{h}}30^{\mathrm{m}}$ (see § 5.3). In particular, in view of these differences, it does not seem to be justified to extrapolate the properties derived in the SMC Wing to the whole Bridge and vice versa, at least not without a better understanding of the connection between these two regions.

The Hα intensity of a cloud can be used to estimate the incident Lyman continuum flux. In our Galaxy, Reynolds (1984, 1993) has used this approach to calculate the power required to ionize the Galactic WIM up to 2–3 kpc above the plane, comparing it with the power available from OB-type stars. Following Tufte et al. (1998), the incident Lyman continuum flux is $F_{\rm LC} = 2.1 \times 10^5 I[{\rm H}\alpha]$ photons s^{-1} cm^{-2}, where $I[{\rm H}\alpha]$ in rayleighs is assumed to arise solely from photoionization. Using the 3 σ upper limit derived from C II*, we find for the diffuse ionized gas of the Bridge (outside denser H II regions around OB-type stars) $F_{\rm LC}({\rm MB}) < 0.4 \times 10^5$ photons s^{-1} cm^{-2}. This rate is at least 100 times smaller than the one found in the Galaxy at high galactic latitudes (Reynolds 1984). This rate would increase by a factor of 4 if we used the C II* detection, but as discussed above, the origin of the excitation is uncertain, as both cold neutral and warm ionized gas could contribute to the observed absorption. We therefore concentrate in this section on the origin of the nearly fully ionized gas.

The flux of Lyman continuum photons from stars is highly dependent on their types (Panagia 1973). For example, an O6-type star will produce a factor of 10 more ionizing photons than an O9. But, more importantly, the rate of photons drops dramatically for B1 and later types: a B1 compared to an O9 produces 600 times fewer ionizing photons per second. In our Galaxy, surveys of OB-type stars have shown that O-type stars produce 93% of ionizing photons, even though they are much less numerous than B-type stars (Terzian 1974; Abbott 1982).

Unfortunately, little is known about the OB-type distribution in the Bridge, especially outside the SMC Wing. Irwin et al. (1990) reported an O8 star outside the SMC Wing, and therefore there are likely to be O-type stars in the Bridge. In the SMC Wing, Pierre et al. (1986) estimated that the number of ionizing photons over a very small area (0.1 deg^2) is 70×10^6 photons s^{-1} cm^{-2}. Such a value would only require 0.1% escaping Lyman continuum photons from the SMC Wing to ionize the Bridge. However, the sample of Pierre et al. (1986) is small and may be not be representative of the OB distribution in the Wing. In particular, 20% of the stars in their sample with types earlier than B0 are O7, which seems to be quite a large number (in our Galaxy this number is about 4%; e.g., Terzian 1974); the three O7 stars in their sample contribute to the majority of ionizing photons. A better characterization of the spectral types of the stars in the SMC Wing and Bridge would clearly help to better understand this important source of ionizing photons.

OB stars in the Bridge and Wing will also create an environment that is favorable for the escape of Lyman continuum photons and for sustaining a high level of ionization throughout the Bridge. Indeed, OB associations through the winds and death of massive stars can produce large bubbles and chimneys that can help ionizing photons travel large distances (e.g., Dove & Shull 1994; Dove et al. 2000; Norman & Ikeuchi 1989). Such H I shells and even possible blowouts and chimneys were surveyed by Muller et al. (2003), but only in the Wing at R.A. $< 3^{\rm h}$, and some may be only due to projection effects (Muller & Bekki 2007). Furthermore, in an overall low-density medium, it is likely that signatures of supernova remnants and stellar winds will be difficult to decipher, since rather than forming shells as observed in dense H I regions, they might just dilute themselves in their surroundings.

Supernovae could also play a role in the ionization of the Bridge. Since stellar formation has occurred for 200–300 Myr (Harris 2007), it is likely that there have been several supernovae in and near the Bridge. Assuming steady ionization of H (with $\sim$13.6 eV per ionization), our limits on Hα require $< 9 \times 10^{-7}$ erg s^{-1} cm^{-2}. Over the entire Bridge (assuming a thickness of 5 kpc), this corresponds to a constant power input to the gas of $< 7 \times 10^{38}$ erg s^{-1}. This power requires a supernova rate of about one every 50,000 yr (see Abbott 1982). The supernova rate is unknown and, as discussed by Reynolds (1984), only a small fraction ($\sim$17%) of the kinetic energy injected into the interstellar medium may be converted into ionizing hydrogen. Yet the presence of young, massive stars and supernovae have likely contributed to the ionization and heating of the Bridge.

Highly ionized gas found in the Bridge (Lehner et al. 2001; Lehner 2002) is an indirect signature of hot gas that is still present in significant amounts (e.g., where the observed high ions are in an interface between the hot and cooler gas) or that was present and is in the process of cooling. Both interfaces and cooling of hot gas can produce photons that may be important sources of photoionization of the environment (Slavin et al. 2000; Borkowski et al. 1990; Knauth et al. 2003). For example, Slavin et al. (2000) modeled the contribution to the photoionization from cooling of hot supernova remnants in the disk of our Galaxy and found that this source was adequate to account for the observed ionization of the Galactic halo. Therefore, supernovae in the Bridge and in the SMC and LMC near the Bridge could not only inject energy and heat the Bridge, but their cooling remnants may also provide a source of ionization.

While the escape of ionizing photons from the SMC Wing could be an important source of ionization, the escape of ionizing photons from the Galactic, LMC, and SMC disks (see Bland-Hawthorn & Maloney 1999; Dove et al. 2000) is also likely to contribute to the ionization of the Bridge. Figure 8 in Putman et al. (2003) shows predicted $I[{\rm H}\alpha]$ near the LMC caused by the escape of ionizing photons from the LMC and the Galactic stellar bulge. The Hα emission estimate produced from the leaking photons of the LMC (and the Galaxy, but the latter is rather negligible) could reach 0.1–0.25 R near the LMC. Thus, such leakage alone is likely an important source of ionizing photons for the Bridge.

While it is not clear which ionizing source is dominant in the Bridge, there appear to be enough photons to maintain the high level of ionization seen in the Bridge. The presence of massive stars in the rarefied environment of the Bridge is likely sufficient in itself for this environment to be largely ionized. Since cooling and recombination times are expected to be longer than in the Galactic environment because the Bridge gas has an extremely low metallicity and density, the ionization is likely to be sustainable for a long time. For example, for a 10^6 K gas with a density of 10^{-3} cm^{-3}, the radiative cooling is $t_{\rm cool} \sim (2{-}3) \times 10^9$ yr for 0.1 solar metallicity (Gnat & Sternberg 2007), about 10 times longer than for a solar metallicity environment. Furthermore, according to Harris (2007), star formation has occurred in the Bridge for the last 200–300 Myr, with a lower rate over the last $\sim$40 Myr. Therefore, several generations of OB stars could have ionized the Bridge over a long time period.

We finally note that the ionization fraction toward DGIK 975 is not only larger than that toward DI 1388, but the gas is also more highly ionized. Lehner (2002) reported the measurements of O VI, Si IV, and C IV toward these stars. In particular, $N_{\rm DGIK\ 975}({\rm O\ VI}) \simeq 13 N_{\rm DI\ 1388}({\rm O\ VI})$, while $N_{\rm DGIK\ 975}({\rm Si\ II}) \simeq 2 N_{\rm DI\ 1388}({\rm Si\ II})$. One can refer to Figure 11 in Lehner (2002) to see the dramatic difference in the O VI absorption profiles toward DI 1388 and DGIK 975. Recently, Lehner & Howk (2007) argued for the presence of outflows and even possibly a hot galactic wind from the LMC. Since DGIK 975 is in the outskirts of the LMC and DI 1388 is farther away from the LMC (see Fig. 1), the larger amount of ambient hot gas toward DGIK 975 might be related to

the outflows from the LMC. Perhaps the feedback processes occurring in the LMC inject energy into the Bridge. We note that the amount of metals incorporated into the Bridge gas from the LMC at large distance must be extremely small, since neither the interstellar nor stellar abundances (-1.2 ± 0.2 dex solar for DGIK 975; see Rolleston et al. 1999; Lee et al. 2005) suggest an increase of the metallicity in this region.

5.2. *Metallicity of the Bridge*

The metallicity of the Bridge is difficult to accommodate with most models of the SMC-LMC-Galaxy interactions (but see below). The present-day low metallicity of the Bridge has, however, a simple explanation in the context of the chemical evolution of the SMC if the Bridge is much older than 200 Myr. Indeed, the bursting model for the star formation rate in the SMC described by Pagel & Tautvaisiene (1998) suggests that its metallicity only slowly increased from -1.4 to -1.1 dex between about 12 and 2.5 Gyr ago. In this model (see also Harris & Zaritsky 2004; Idiart et al. 2007), it is only in the last $\sim$2.5 Gyr that the SMC metallicity has exceeded the modern Bridge value. This is a large window for forming the Bridge from SMC gas and suggests that the Bridge could be 10 times older than current *N*-body simulations suggest. Harris (2007) showed that there were several bursts (2.5, 0.4, and 0.06 Gyr ago) of star formation in the SMC in the last $\sim$3 Gyr, but the most important one was 2.5 Gyr ago. New bursts of star formation are believed to often be caused by the effects of close tidal interactions between galaxies (e.g., Larson & Tinsley 1978; Barton et al. 2007). While Harris (2007) noted that the bursts at 2.5 and 0.4 Gyr are temporally coincident with past perigalactic passages of the SMC and Galaxy, these epochs also correspond to close encounters between the SMC and LMC (Kallivayalil et al. 2006a). Due to its proximity, the LMC tidal perturbations on the SMC are larger than those of the Galaxy (Lin et al. 1995). However, calculations of the orbits of the SMC and LMC with the updated proper motions of the SMC and LMC still predict two more perigalactic approaches between the SMC and LMC after the 2.2 Gyr close encounter, at $\sim$1.4 and 0.2 Gyr, the latter being the closest approach (Kallivayalil et al. 2006a). It is therefore unclear whether the Bridge could be stable over 2–3 Gyr (Gardiner & Noguchi [1996] argued that it could not be stable over a very long time, principally because of the Galaxy's gravitational field, yet they did not quantify it further).

On the other hand, Gardiner & Noguchi (1996) predicted from their model that the Bridge gas originated primarily from the halo of the SMC, not its disk. Under the assumption that the tidal models are correct, this would mean that despite the steep increase of star formation rate in the SMC disk, the metallicity of the SMC halo would not have been enhanced in the last 2.5 Gyr by any disk material via outflows or else was diluted by an external low-metallicity source. Assuming that the initial mass of the Bridge is $M^i_{\rm MB}$ and the metallicity is $Z^i_{\rm MB}$, and that there is a "diluting" gas with $M_{\rm dil}$ and $Z_{\rm dil}$, the metallicity of the mixed-up gas in the Bridge, $Z^f_{\rm MB}$, can be expressed as

$$Z^f_{\rm MB} = \frac{Z^i_{\rm MB} M^i_{\rm MB} + Z_{\rm dil} M_{\rm dil}}{M^i_{\rm MB} + M_{\rm dil}}; \quad (3)$$

and assuming that $Z^i_{\rm MB} M^i_{\rm MB} \gg Z_{\rm dil} M_{\rm dil}$, we have

$$Z^f_{\rm MB} = Z^i_{\rm MB} \left(1 + \frac{M_{\rm dil}}{M^i_{\rm MB}}\right)^{-1}. \quad (4)$$

Therefore, if the metallicity of the tidally disrupted material was present-day SMC-like, $Z^i_{\rm MB} = 0.25\ Z_\odot$, one would need $M_{\rm dil} \approx 2M^i_{\rm MB}$ (with $Z_{\rm dil} \lesssim 0.01\ Z_\odot$) to achieve $Z^f_{\rm MB} \approx 0.09\ Z_\odot$. In contrast, $Z^i_{\rm MB} M^i_{\rm MB} \ll Z_{\rm dil} M_{\rm dil}$, $Z^i_{\rm dil} = 0.09\ Z_\odot$, and $Z^i_{\rm MB} = 0.25\ Z_\odot$ would require $M_{\rm dil} \gtrsim 200 M^i_{\rm MB}$ to have $Z^f_{\rm MB} = 0.09\ Z_\odot$. A determination of the ratio of the SMC halo to the SMC disk particles that were pulled into the Bridge in simulations would be valuable. This scenario might be plausible, since dwarf galaxies can have H I gas occupying radii much larger than the stellar component (Salpeter & Hoffman 1996). This scenario was also proposed by Harris (2007) to explain the absence of evidence of tidally stripped stars in the Bridge. If this envelope was extended enough, it could have reduced the impact of feedback from massive stars in the SMC at large distances from the SMC for $\sim$2–3 Gyr.

If the very low metallicity material did not come from an extended halo of gas around the SMC stellar disk (and assuming the Bridge is young), the Bridge could have swept up metal-poor ambient matter over time. For example, measurements of the proper motion of the Fornax dwarf spheroidal galaxy suggest that the orbit of the Magellanic Clouds was crossed by Fornax some 200 Myr ago (Dinescu et al. 2004), a time coincidentally similar to the believed formation epoch of the Bridge. Fornax has a wide range of metallicity, from -2.0 to -0.4 dex solar, and a peak near -0.9 dex (Pont et al. 2004). While this is speculative, low-metallicity material from Fornax or other sources may have mixed with Bridge gas.

Bekki & Chiba (2007a, 2007b) have recently produced self-consistent chemodynamical models of the LMC-SMC-Galaxy interactions and found a metallicity distribution that peaks at -0.8 dex but could extend down to -0.9 dex. To the best of our knowledge, this is the only model that attempts to explain the lower metallicity of the Bridge. In this model, a low metallicity is reached because the Bridge is mostly formed from the SMC halo gas, where the metallicity is significantly smaller because of an assumed metallicity gradient in the SMC, although it is not clear that there is or has been such a gradient, since the present-day metallicity in the SMC Wing (Lee et al. 2005) is similar to the SMC.

5.3. *Concluding Remarks*

Our analysis provides the first metallicity of the Bridge gas and shows for the first time that the Bridge is substantially ionized. As our sample of sight lines is small, it is, however, not certain whether large chemical and/or ionization inhomogeneities exist. As we argued above, our three sight lines probe the low H I column density regions of the Bridge (R.A. $\gtrsim 3^{\rm h}$) at very different locations and depths. The present-day metallicity of the Bridge derived from three B-type stars (including DGIK 975) also suggests some chemical homogeneity (Rolleston et al. 1999; Lee et al. 2005). We note that two of the Rolleston et al. stars are close to the SMC Wing but outside the high H I column density regions. In contrast, Lee et al. (2005) found an SMC-like metallicity for four B-type stars well inside the SMC Wing (and in the high H I column density region of the Wing). While the samples are small in each region, it seems unlikely that each of the current samples probes an unrepresentative population.

The difference of 0.4–0.5 dex in the metallicity between these two adjacent regions is another puzzle, although we note that Lee et al. (2005) quoted errors of $\pm$0.3 dex in their abundances and the difference may actually be smaller. These authors also used the same method for the SMC Wing and Bridge stars and found a systematic difference of about 0.5 dex in the abundance of these stars. This difference may be explained (assuming that chemical

inhomogeneities in each region are small) if the Wing and the low H I column density regions of the Bridge have different origins, the star formation rate and initial mass function were quite different in each region, and/or the Wing was not diluted with extremely low metallicity gas. In the first scenario, the Wing must be younger than the rest of the Bridge, so that it was formed recently from gas and stars stripped from the SMC that have a present-day SMC metallicity. This would imply that the Bridge itself must be much older and that the star formation was inefficient over a long period of time or only started in the last 200–300 Myr, as the results of Harris (2007) suggest. In the second scenario, at the epoch in which the Bridge and the Wing were formed, the metallicity should have been around $\lesssim -1.1$ dex in both regions. However, it would seem very unlikely that the metallicity of the Wing has increased by 0.5 dex in the last 200 Myr, assuming this is the age of these structures. In the SMC, where star formation is more important than in the Wing, about 2–3 Gyr were needed to increase the metallicity from -1.1 dex to the present-day metallicity (Pagel & Tautvaisiene 1998). Therefore, the second scenario is not likely if these structures are only 200 Myr old. In the third scenario, the Bridge outside the Wing regions could have been diluted with low-metallicity gas, while the Wing was not or was at a negligible level, possibly because the star formation was more efficient or the Wing material came from deeper regions of the SMC (where the gas has present-day SMC metallicity) than the rest of the Bridge gas. The first and third scenarios are consistent with the findings of evolved stars in the Wing and not in the Bridge (Harris 2007).

Hence, despite the fact that current tidal simulations reproduce well the observed H I structures (i.e., the Bridge, Stream, and Leading Arm), they seem to be in conflict with the above conclusions regarding the metallicities. As already mentioned, the velocities of the LMC and SMC adopted in the models of Gardiner & Noguchi (1996) and subsequent models differ from those derived from the recent proper-motion estimates of the SMC and LMC by over 100 km s^{-1} (Kallivayalil et al. 2006a, 2006b). It is also unclear how bound the SMC and LMC are and were (Kallivayalil et al. 2006a). With those updated proper motions, Besla et al. (2007) strongly suggest that existing numerical models of the Clouds may no longer be appropriate and, in particular, cannot explain the Stream and Leading Arm. As discussed by Nidever et al. (2008), current simulations may also miss important physics, including feedback processes such as outflows from the LMC that may interact with the Bridge gas. In particular, it is quite important to understand feedback and mixing processes in the SMC disk and halo for the last 3 Gyr if the Bridge is only 200 Myr old and its main origin is the halo of the SMC.

Future theoretical investigations using the updated proper motions of the LMC and SMC should not only try to reproduce the H I properties but also accommodate the low metallicity of the Bridge, the apparent discrepancy of the metallicity between the Bridge and the SMC Wing, its ionization structure, and the apparent lack of old stars in the Bridge (Harris 2007). Future models should, in particular, investigate whether the Bridge can be stable over a long time (2–3 Gyr) or, despite an important burst of star formation within the SMC 2.5 Gyr ago, the SMC halo gas could maintain a very low metallicity. If none of these conditions are satisfied, an important (depending on the chemical homogeneity in the Bridge) amount of matter in the Bridge must come from somewhere else. If the Bridge could survive several perigalactic approaches between the SMC and LMC, it would be interesting to know whether the low-density and low-metallicity regions of the Bridge could have been formed some 2–3 Gyr ago, while the SMC Wing would have been produced at a later time, some 200 Myr ago, during the last and closest approach between the SMC and LMC.

From an observational point of view, a larger stellar and interstellar sample in which the abundances could be estimated in the Bridge and the SMC Wing would be extremely valuable. The soon-to-be-installed Cosmic Origins Spectrograph (COS) will be particularly useful for the study of the gas phases in the Bridge, since fainter targets can be observed with it. In particular, to better characterize the ionization structure, future COS and deep Hα observations will be invaluable. A better characterization of the stellar population in the Bridge will also help constrain the origin of the ionization, the star formation history, and the initial mass function in the Bridge. Since the Bridge is the closest gaseous and stellar tidal remnant, and since interactions between galaxies are rather common, future observational and theoretical efforts offer a unique opportunity to comprehend the physical processes and origin of such structures.

6. SUMMARY

Using far-UV spectra obtained with *FUSE* and the *HST* STIS E140M, we analyze the physical properties and abundances of the Magellanic Bridge gas toward three sight lines that are situated at different locations in the Bridge and probe various depths. These observations provide access to neutral and ionized species at sufficient signal-to-noise ratio and resolution to estimate their column densities and kinematics. In Table 5 we summarize the abundances and physical properties of the Bridge determined from our investigation. Our main findings are as follows:

1. Toward one sight line, we find that the Bridge metallicity is $[Z/\mathrm{H}] = -1.02 \pm 0.07$, and toward another we find $-1.7 < [Z/\mathrm{H}] < -0.9$. To derive these quantities we compare the column densities of neutral elements (O I, Ar I, and N I) to that of H I. The metallicity of the gas in the Bridge is in excellent agreement with the average metallicity determined in B-type stars. There is some evidence that N might be less deficient than usually observed in gas with $[Z/\mathrm{H}] \approx -1$ and even possibly not deficient with respect to O.

2. The very low present-day metallicity in the Bridge is similar to the SMC before a burst of star formation that occurred about 2.5 Gyr ago. This may not only be pure coincidence, since interactions between galaxies are believed to create bursts of star formation within the interacting galaxies. Yet, it is unclear at this time whether the Bridge could survive subsequent perigalactic passages of the LMC with the SMC. Hence, the Bridge could be much younger, as currently predicted by tidal models. In this case, it would require a high level of dilution with an unidentified component with extremely low metallicity; this component would have to be dominant in order to reach the present-day Bridge metallicity.

3. We determine that the gas of the Bridge is largely ionized toward our three sight lines, with only $\sim$20% of the gas being neutral, implying that the largest fraction of the gas mass of the Bridge comes from the ionized gas. Toward two sight lines, we find that there are at least two main components in absorption, and the component with the lower velocity is systematically more ionized. We argue that possible sources for the ionization are the hot stars within and near the Bridge, hot gas (indirectly detected via O VI absorption), and photons leaking from the SMC, LMC, and Milky Way.

4. From the analysis of C II*, we find $n_e < 0.03\sqrt{T_4}$ cm^{-3} in the nearly fully ionized gas and $n_e < 0.1\sqrt{T_4}$ cm^{-3} in the partially ionized gas. Since the gas is dominantly ionized, our analysis suggests that the overall density of the Bridge gas is extremely

low. This is consistent with the absence of detection of Hα emission in the diffuse gas of the Bridge with current observations. Denser and less dense regions must also exist in the Bridge on account of the multiphase (cooler and hotter gas) nature of the Bridge.

We thank the anonymous referee for constructive comments that improved and strengthened the content of our manuscript. As this paper was submitted, *FUSE* abruptly failed permanently. We want to express our gratitude to the *FUSE* science, hardware, and mission-operation teams for providing high-quality FUV spectroscopic data for the last 8 years. Support for this research was provided by NASA through grants FUSE-NNX06F42G and FUSE-NNX07AK09G. F. P. K. is grateful to AWE Aldermaston for the award of a William Penney Fellowship. This research has made use of the NASA Astrophysics Data System Abstract Service and the Centre de Données de Strasbourg (CDS).

REFERENCES

Abbott, D. C. 1982, ApJ, 263, 723
Aguirre, A., Hernquist, L., Schaye, J., Katz, N., Weinberg, D. H., & Gardner, J. 2001, ApJ, 561, 521
Asplund, M., Grevesse, N., & Sauval, A. J. 2006, Commun. Asteroseis., 147, 76
Bajaja, E., Arnal, E. M., Larrarte, J. J., Morras, R., Pöppel, W. G. L., & Kalberla, P. M. W. 2005, A&A, 440, 767
Barnes, J. E., & Hernquist, L. 1992, ARA&A, 30, 705
Barton, E. J., Arnold, J. A., Zentner, A. R., Bullock, J. S., & Wechsler, R. H. 2007, ApJ, 671, 1538
Battinelli, P., & Demers, S. 1992, AJ, 104, 1458
Bekki, K., & Chiba, M. 2007a, Publ. Astron. Soc. Australia, 24, 21
———. 2007b, MNRAS, 381, L16
Besla, G., Kallivayalil, N., Hernquist, L., Robertson, B., Cox, T. J., van der Marel, R. P., & Alcock, C. 2007, ApJ, 668, 949
Bica, E. L. D., & Schmitt, H. R. 1995, ApJS, 101, 41
Bland-Hawthorn, J., & Maloney, P. R. 1999, ApJ, 510, L33
Borkowski, K. J., Balbus, S. A., & Fristrom, C. C. 1990, ApJ, 355, 501
Brüns, C., et al. 2005, A&A, 432, 45
Cardelli, J. A., Meyer, D. M., Jura, M., & Savage, B. D. 1996, ApJ, 467, 334
de Mello, D. F., Smith, L. J., Sabbi, E., Gallagher, J. S., Mountain, M., & Harbeck, D. R. 2008, AJ, 135, 548
Demers, S., & Battinelli, P. 1998, AJ, 115, 154
Dinescu, D. I., Keeney, B. A., Majewski, S. R., & Girard, T. M. 2004, AJ, 128, 687
Diplas, A., & Savage, B. D. 1991, ApJ, 377, 126
Dixon, W. V., et al. 2007, PASP, 119, 527
Dove, J. B., & Shull, J. M. 1994, ApJ, 430, 222
Dove, J. B., Shull, J. M., & Ferrara, A. 2000, ApJ, 531, 846
Gardiner, L. T., & Noguchi, M. 1996, MNRAS, 278, 191
Gnat, O., & Sternberg, A. 2007, ApJS, 168, 213
Grevesse, N., & Sauval, A. J. 1998, Space Sci. Rev., 85, 161
Harris, J. 2007, ApJ, 658, 345
Harris, J., & Zaritsky, D. 2004, AJ, 127, 1531
Henry, R. B. C., & Prochaska, J. X. 2007, PASP, 119, 962
Howk, J. C., Savage, B. D., & Fabian, D. 1999, ApJ, 525, 253
Howk, J. C., Sembach, K. R., & Savage, B. D. 2006, ApJ, 637, 333
Idiart, T. P., Maciel, W. J., & Costa, R. D. D. 2007, A&A, 472, 101
Irwin, M. J., Demers, S., & Kunkel, W. E. 1990, AJ, 99, 191
Jenkins, E. B., et al. 2000, ApJ, 538, L81
Kalberla, P. M. W., Burton, W. B., Hartmann, D., Arnal, E. M., Bajaja, E., Morras, R., & Poumlppel, W. G. L. 2005, A&A, 440, 775
Kallivayalil, N., van der Marel, R. P., & Alcock, C. 2006a, ApJ, 652, 1213
Kallivayalil, N., van der Marel, R. P., Alcock, C., Axelrod, T., Cook, K. H., Drake, A. J., & Geha, M. 2006b, ApJ, 638, 772
Knauth, D. C., Howk, J. C., Sembach, K. R., Lauroesch, J. T., & Meyer, D. M. 2003, ApJ, 592, 964
Kobulnicky, H. A., & Dickey, J. M. 1999, AJ, 117, 908
Larson, R. B., & Tinsley, B. M. 1978, ApJ, 219, 46
Lee, J.-K., Rolleston, W. R. J., Dufton, P. L., & Ryans, R. S. I. 2005, A&A, 429, 1025
Lehner, N. 2002, ApJ, 578, 126
Lehner, N., & Howk, J. C. 2007, MNRAS, 377, 687
Lehner, N., Jenkins, E. B., Gry, C., Moos, H. W., Chayer, P., & Lacour, S. 2003, ApJ, 595, 858
Lehner, N., Sembach, K. R., Dufton, P. L., Rolleston, W. J. R., & Keenan, F. P. 2001, ApJ, 551, 781
Lehner, N., Wakker, B. P., & Savage, B. D. 2004, ApJ, 615, 767
Lin, D. N. C., Jones, B. F., & Klemola, A. R. 1995, ApJ, 439, 652
Maller, A. H., Katz, N., Kereš, D., Davé, R., & Weinberg, D. H. 2006, ApJ, 647, 763
Mathewson, D. S., Cleary, M. N., & Murray, J. D. 1974, ApJ, 190, 291
Meyer, D. M., Cardelli, J. A., & Sofia, U. J. 1997, ApJ, 490, L103
Meyer, D. M., Jura, M., & Cardelli, J. A. 1998, ApJ, 493, 222
Mizuno, N., Muller, E., Maeda, H., Kawamura, A., Minamidani, T., Onishi, T., Mizuno, A., & Fukui, Y. 2006, ApJ, 643, L107
Morton, D. C. 2003, ApJS, 149, 205
Muller, E., & Bekki, E. 2007, MNRAS, 381, L11
Muller, E., & Parker, Q. 2007, Publ. Astron. Soc. Australia, 24, 69
Muller, E., Staveley-Smith, L., & Zealey, W. J. 2003, MNRAS, 338, 609
Nidever, D. L., Majewski, S. R., & Burton, W. B. 2008, ApJ, in press (arXiv: 0706.1578)
Norman, C. A., & Ikeuchi, S. 1989, ApJ, 345, 372
Oliveira, C. M., Dupuis, J., Chayer, P., & Moos, H. W. 2005, ApJ, 625, 232
Pagel, B. E. J., & Tautvaisiene, G. 1998, MNRAS, 299, 535
Panagia, N. 1973, AJ, 78, 929
Pierre, M., Viton, M., Sivan, J. P., & Courtes, G. 1986, A&A, 154, 249
Pont, F., Zinn, R., Gallart, C., Hardy, E., & Winnick, R. 2004, AJ, 127, 840
Putman, M. E. 2000, Publ. Astron. Soc. Australia, 17, 1
Putman, M. E., Bland-Hawthorn, J., Veilleux, S., Gibson, B. K., Freeman, K. C., & Maloney, P. R. 2003, ApJ, 597, 948
Reynolds, R. J. 1984, ApJ, 282, 191
———. 1993, in AIP Conf. Proc. 278, Back to the Galaxy, ed. S. S. Hold & F. Verter (Melville: AIP), 156
Rolleston, W. R. J., Dufton, P. L., McErlean, N. D., & Venn, K. A. 1999, A&A, 348, 728
Russell, S. C., & Dopita, M. A. 1992, ApJ, 384, 508
Salpeter, E. E., & Hoffman, G. L. 1996, ApJ, 465, 595
Savage, B. D., & Sembach, K. R. 1991, ApJ, 379, 245
Sembach, K. R., & Savage, B. D. 1992, ApJS, 83, 147
Slavin, J. D., McKee, C. F., & Hollenbach, D. J. 2000, ApJ, 541, 218
Sofia, U. J., & Jenkins, E. B. 1998, ApJ, 499, 951
Terzian, Y. 1974, ApJ, 193, 93
Tufte, S. L., Reynolds, R. J., & Haffner, L. M. 1998, ApJ, 504, 773
Wakker, B. P., Kalberla, P. M. W., van Woerden, H., de Boer, K. S., & Putman, M. E. 2001, ApJS, 136, 537
Welty, D. E., Lauroesch, J. T., Blades, J. C., Hobbs, L. M., & York, D. G. 1997, ApJ, 489, 672
Wolfire, M. G., McKee, C. F., Hollenbach, D., & Tielens, A. G. G. M. 1995, ApJ, 453, 673
———. 2003, ApJ, 587, 278
Yoshizawa, A. M., & Noguchi, M. 2003, MNRAS, 339, 1135